Electronic Supplementary Material (ESM)
Solutions, Ag/AgCl electrodes, Ion activity calculations, Extra Figures and Data tables

An optimised 3M KCl salt-bridge technique to measure and validate theoretical liquid junction potential values in patch-clamping by Peter H Barry, Trevor M. Lewis and Andrew J. Moorhouse

This electronic supplementary material is to accompany the above article (Barry et al., 2013; DOI 10.1007/s00249-013-0911-3).

Salts and solutions

The NaCl (99.9% purity) and KCl (99.8% purity), Analytical Grade, came from Ajax Finechem (www.ajaxfinechem.com). The CsCl (99.9% purity) came from Sigma-Aldrich and was stored in an electrical dessicator (Secador, John Morris Scientific P/L) prior to use. Because of the hygroscopic nature of LiCl and the humidity of the laboratory, LiCl solutions were made up from commercial 8M LiCl solutions (Sigma_Aldrich; Molecular Biology Grade, ≥ 99%; checked by Sigma using $AgNO_3$ titration) which were first diluted to 400 mM stock solution and then further diluted volumetrically to their final concentrations. The NaI and NaF salts also came from Sigma-Aldrich and were ≥ 99% pure.

Production of Ag/AgCl electrodes

For the XCl electrode-salt bridge combination, where X refers to the alkali cations, Li^+, Na^+, K^+ or Cs^+, the Ag/AgCl electrode was made from sterling Ag wire electroplated in 0.1 M HCl. The Ag wire was physically cleaned with fine wet-and-dry sandpaper (400 grit) and handled with rubber gloves to avoid getting any grease from fingers on it. It was then washed in reverse osmosis (RO) water and dried with laboratory wipes. A few Ag wires (1-3 at a time) were then chlorided in 0.1 M HCl by passing unidirectional current between them (as the anode) and a second Ag electrode as the cathode, at fairly low current density 1-10 $mA.cm^{-2}$ for a number of minutes until the electrodes became a uniform mauve-brown. The Ag/AgCl wires are then washed in RO water. Note that reversing the current during electroplating is not recommended for making good potential measuring electrodes (e.g., Ives and Janz, 1961).

One of the Ag/AgCl wires is then placed in a modified glass Pasteur pipette, with a major part of the fine end of the pipette removed and the tip heat-polished, and the non-chlorided end of the Ag wire taped with a strip of plastic insulating tape to the outside of the pipette to hold it in place, as shown in Fig. S1. The pipette is then filled by syringe, from the larger diameter end, with a simple molten 150 mM XCl solution to which about 4% agar has been added (%wt/vol, i.e., ~4 g/100 ml; with the agar previously dissolved in the XCl by bringing it slowly to the boil) and allowed to cool and gell. The pipette is then sealed at the air-Ag/AgCl-agar-salt interface by a silicon rubber compound (Sylgard, Dow Corning) to minimize electrode deterioration and the electrode stored in a container with 150 mM XCl.

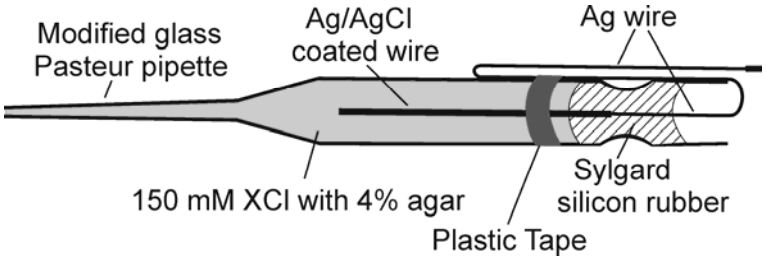

Fig. S1. *A schematic diagram of a 150 mM XCl Ag/AgCl electrode made from a modified glass Pasteur pipette and used for the measurements in the accompanying paper.*

The potential V_e of the Ag/AgCl single junction electrode is given by:

$$V_e = V_o^{Ag} - (RT/F) \ln (a_{Cl}) \quad \text{(S1)}$$

Where V_e represents the potential of the electrode with respect to the solution, V_o^{Ag} represents the standard electrode potential of the electrode and a_{Cl} the activity of Cl^- in the gelled solution in the electrode, and R, T and F have their usual significance of gas constant, Temp in K and Faraday.

Ion activity calculations

In order to determine the activity of ions in the solutions, it is necessary to determine first the ionic strength of the solutions, *I*, taking into account the contribution of all monovalent and divalent ions. *I* will be determined from the equation:

$$I = \sum_i \frac{C_i z_i^2}{2} \quad \text{(S2)}$$

where C_i is the concentration of each ion i in the solution and z_i is their valency. Given the relatively small proportion of ions like $HEPES^-$ and Ca^{2+} ions in the predominantly XCl solutions, where X represents the predominant cation in the solution (e.g., Na^+, K^+, Li^+ or Cs^+), the activity coefficient was taken from published data. In order to calculate individual ion activities, it can also be reasonably assumed that the interionic forces affect anion and cation equally and hence that the Guggenheim assumption should apply (MacInnes, 1961), which indicates that for a uni-univalent electrolyte, the individual ion activity coefficients (γ) will be the same, so that, for example, in an NaCl solution $\gamma_{Na} = \gamma_{Cl}$. In each case, the ion activity, a, will be related to the ion concentration, C, by:

$$a = \gamma C \quad \text{(S3)}$$

Estimates of ionic strength for some NaCl solutions are later shown in Table 1.

LiCl solutions. Likewise, the published activity data (between 10 and 200 mM) of Robinson & Stokes 1965; Table 9 of Appendix 8.7) at the temperature of the solution freezing point (within 0.2 % of the value at 25 ^oC for 100 mM; Table 9 of Appendix 8.10) was used by Barry et al. (2010) to show that the activity coefficients (γ) in LiCl solutions are fitted by the following relationship:

$$\gamma = 0.9895 - 0.9659x + 1.0232x^2 \quad \text{(S4)}$$

where $x = \sqrt{m}$ LiCl, and m is the molal concentration of LiCl, and is approximated by I, so that $x \cong \sqrt{I}$. For simplicity, m was approximated by molar (M) concentrations, the errors generally being less than 0.2% and the relative errors in final activities being much less than this.

NaCl solutions. The published activity data (between 20 and 200 mM) of Robinson & Stokes (1965; Table 1 of Appendix 8.9 and Table 10 of Appendix 8.1) at 25 ^oC was fitted using SigmaPlot by Sugiharto et al.(2010) to show that the activity coefficients (γ) in NaCl solutions are fitted by the following relationship:

$$\gamma = 0.9907 - 0.940x + 0.830x^2 \quad \text{(S5)}$$

where $x = \sqrt{m}$ NaCl, and is similarly approximated by $\sqrt{I}$, as in the case of LiCl above.

KCl solutions. Similarly, the published activity data (between 20 and 190 mM) of Robinson & Stokes (1965; Table 1, Appendix 8.9 and Table 11, Appendix 8.10) at 25 ^oC was used by Barry et al. (2010) to show that the activity coefficients (γ) in KCl solutions are fitted by the following relationship:

$$\gamma = 0.9908 - 0.9464x + 0.7586x^2 \quad \text{(S6)}$$

where $x = \sqrt{m}$ KCl, is similarly approximated as $\sqrt{I}$.

CsCl solutions. Similarly, the published activity data (between 17 and 193 mM) of Cui et al. (2007) at 25 ^{o}C was used by Barry et al. (2010) to show that the activity coefficients (γ) in CsCl solutions are fitted by the following relationship:

$$\gamma = 0.9814 - 0.9107x + 0.6105x^2 \quad \text{(S7)}$$

where $x = \sqrt{m}$ CsCl, is similarly approximated as $\sqrt{I}$. Note that the equivalent equation given in the above paper was for an extended concentration range, although the values used in their tables were the more accurate figures fitted over the limited range using the parameters of Eq. S7, as used in this present paper.

NaI solutions. The published activity data (between 100 and 400 mM) of Robinson & Stokes (1965; Table 11, Appendix 8.10) at 25 ^{o}C were used to show that the activity coefficients (γ) in NaI solutions are fitted by the following relationship:

$$\gamma = 0.9353 - 0.6095x + 0.4435x^2 \quad \text{(S8)}$$

where $x = \sqrt{m}$ NaI, is similarly approximated as $\sqrt{I}$.

NaF solutions. The published activity data (between 100 and 400 mM) of Robinson & Stokes (1965; Table 11, Appendix 8.10) at 25 ^{o}C were used to show that the activity coefficients (γ) in NaI solutions are fitted by the following relationship:

$$\gamma = 0.9403 - 0.6519x + 0.3080x^2 \quad \text{(S9)}$$

where $x = \sqrt{m}$ NaF, is similarly approximated as $\sqrt{I}$.

3M KCl Solution. The activity coefficient of 3M KCl was obtained from published data at 25 ^{o}C to be 0.5690 (Robinson and Stokes, 1965; Table 11, Appendix 8.10), to give an activity for 3M KCl of 1707 mM.

Data Tables

Table S1. Sample table of ion activities for the NaCl dilution experiments

Solution	Ion Conc. (mM)	I (M)	$\sqrt{I}$ ($\sqrt{M}$)	(γ)	a (mM)	$HEPES^-$ (C)	$HEPES^-$ (a)
1.0 Na_o	149.3	0.1500	0.3873	0.7511	112.1	4.3	3.2
0.5 Na_o	79.3	0.0800	0.2828	0.7912	62.7	4.3	3.4
0.25 Na_o	41.7	0.0425	0.2062	0.8322	34.7	4.2	3.5
1.0 Cl_o	145.0	0.1500	0.3873	0.7511	108.9	4.3	3.2
0.5 Cl_o	75.0	0.0800	0.2828	0.7912	59.3	4.3	3.4
0.25 Cl_o	37.5	0.0425	0.2062	0.8322	31.2	4.2	3.5

NaOH concentrations added were 4.3, 4.3 and 4.2 mM for the 1.0 NaCl, 0.5 NaCl and 0.25 NaCl solutions respectively. 136 mM and 189 mM sucrose were added to the 0.5 NaCl and 0.25 NaCl solutions respectively to keep them approximately isoosmotic.

Note that for the recent NaCl biionic experiments, 4.5 mM NaOH needed to be added during the 1.0 NaCl solution buffering, so that an additional 4.5 mM Na^+ ions were allowed for to give a Na^+ concentration of 149.5 mM and activity of 112.3, and a $HEPES^-$ concentration of 4.5 and activity of 3.4.

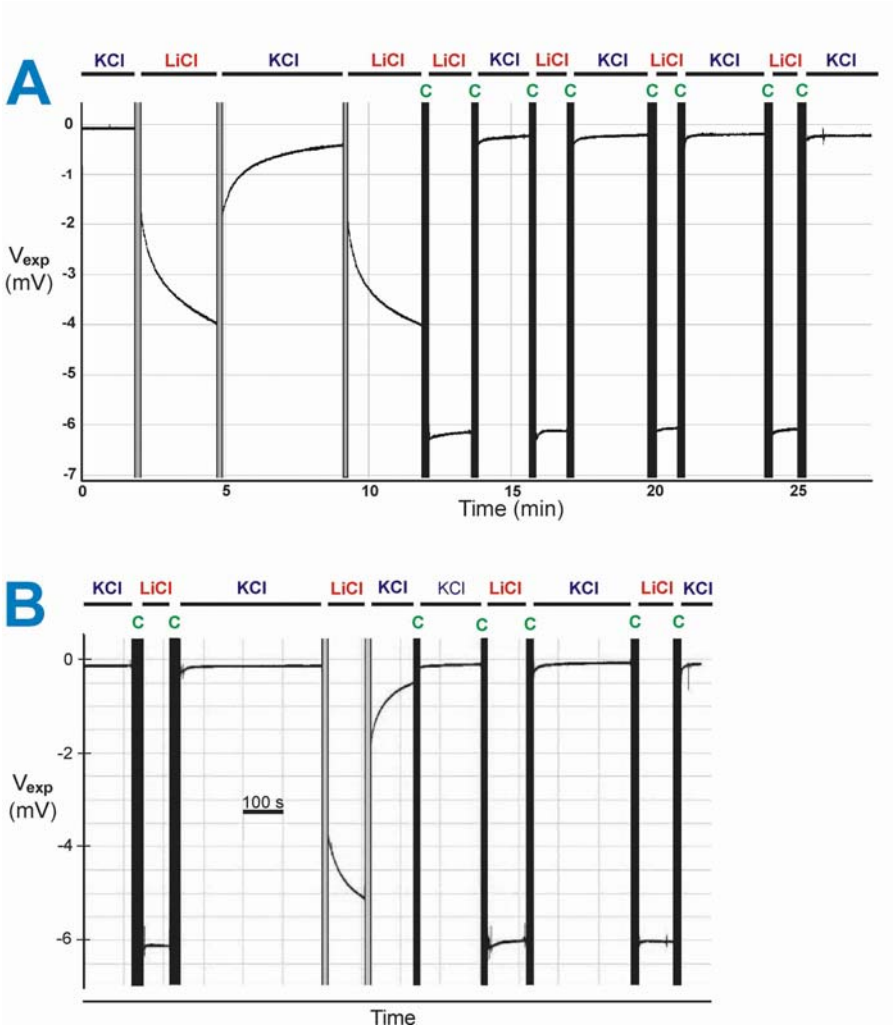

Fig. S2. *Two experimental records to illustrate the necessity of cutting off the tip of the 3M KCl salt-bridge whenever it is transferred to a new solution with different composition (or concentration). The records show the voltage potentials measured between two agar bridge electrodes, a ~150 mM KCl salt-bridge (initially equilibrated with the 145 mM KCl solution) and a 3M KCl reference salt-bridge, both placed in a control (1.0 KCl with 145 mM KCl) or test (1.0 LiCl with 145 mM LiCl) solution as indicated (see setup in Fig. 1 in main paper). The solid bar above each of the traces indicates when the test solution was changed from the 145 mM KCl beaker (KCl) to the 145 mM LiCl beaker (LiCl). The resultant shifts in these junction potentials shown represents the shifts in the sum of the LJPs at the two salt-bridge interfaces. The grey vertical bars on the trace indicate the time during which the solution changeover takes place when the 3M KCl salt-bridges is not cut, and the black vertical bars (and green 'C' above) indicate the time during the solution changeover when the end of the 3M KCl salt-bridge is cut off by at least 6 mm before just before the solution change. In Panel A, the salt-bridges had equilibrated for about 2 hours in the standard 145 mM KCl solution, which allowed the end of the 3M KCl salt-bridge to be replaced in large part by the 145 mM KCl solution. Solution changes then resulted in slow transient responses well below the value expected with a fresh 3M KCl salt-bridge. As soon as that salt-bridge is cut off (this first time by about 2 cm) and the salt-bridges transferred to the LiCl solution, the potential immediately jumps to the maximum value. Subsequent solution changes with a freshly-cut 3M KCl salt-bridge also rapidly jump between the maximum test and control values, as can be clearly seen. Panel B shows a separate experiment illustrating that even a short 6 min equilibration in the KCl solution results in truncated slow transient responses when the solution is changed without the 3M KCl bridge being cut.*

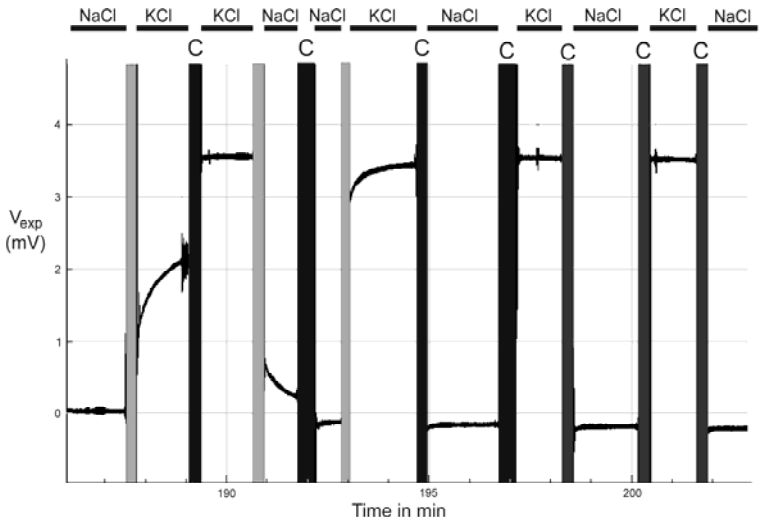

Fig. S3. *The chart record of an experiment in which the freshly-cut tip of a 3M KCl salt-bridge was initially left in the 145 mM NaCl control solution for 120 min to allow the salt-bridge composition to equilibrate with that of the control solution. The bath solution was then changed to 145 mM KCl (as depicted in the horizontal bar above the charts) to record a shift in V_{LJ}, with the salt-bridge not being cut for that solution change (as depicted by a gray vertical bar). Other solution changes and/or salt-bridge cuts are shown by the vertical black bars with a 'C' above them, to indicate the cutting of the end of the 3M KCl salt-bridge by 10 mm (for the first 3 cuts) and then 8-10 mm cuts for the remainder. The first 3 salt-bridge cuts were 10 mm in length and the remainder between 8-10 mm. The figure indicates that after three 10 mm cuts off the end of the salt-bridge, the shift in V_{exp} had reached a maximum value and was no longer transient in time course.*

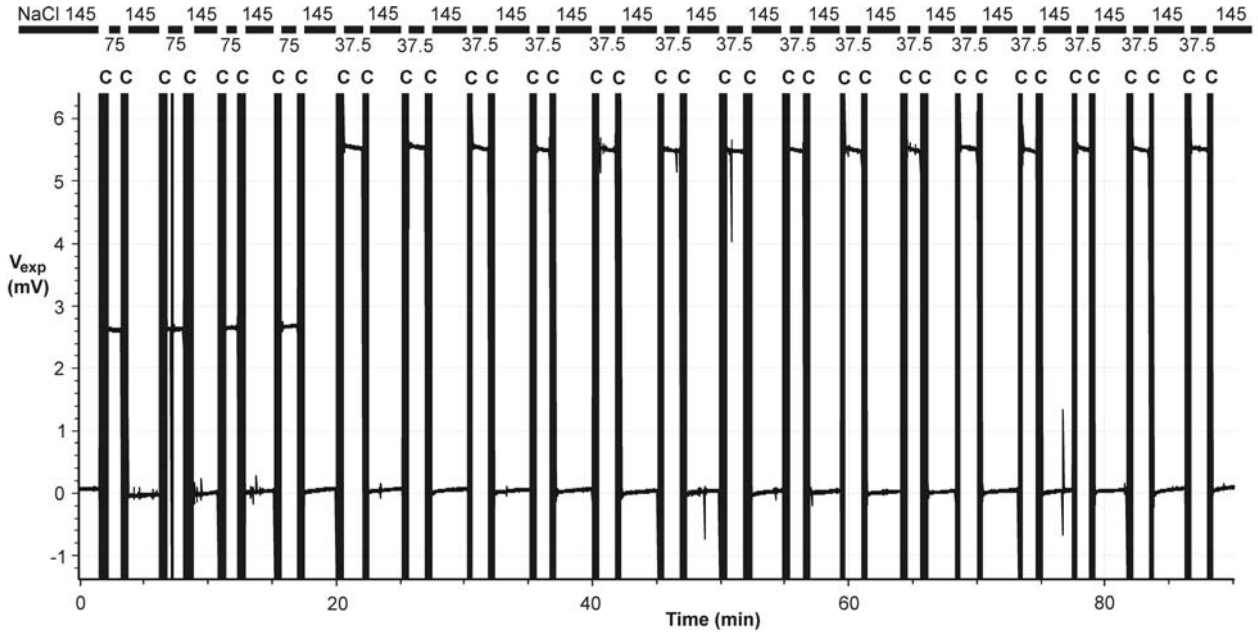

Fig. S4. *Another example of the consistent and rapid rectangular shifts in liquid junction potentials measured for solution dilutions, in this case from 1.0 NaCl to 0.5 NaCl (145 mM to 75 mM NaCl; the first four solution changes) and from 1.0 NaCl to 0.25 NaCl (145 mM to 37.5 mM NaCl; the remainder) at 22°C. See Fig. 1 (main paper) for experimental setup, and* ***Solutions*** *section for full details of solution compositions. Again the LJPs are measured as the difference between a 150 mM NaCl agar salt-bridge (initially equilibrated with a 1.0 NaCl solution) and a 3M KCl reference salt-bridge, when the 3M KCl salt-bridge tip is cut off just prior to every solution transfer. The black vertical bars (and 'C's) indicate the period during which the solution is changed and the tip of the 3M KCl reference salt-bridge was cut, thereby having a fresh 3M KCl interface in contact with the new solution.*

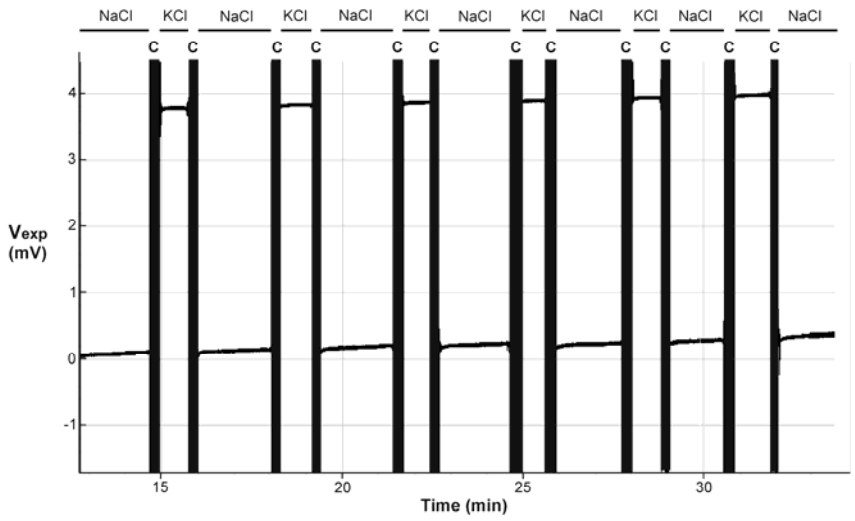

Fig. S5. *An example of the consistent and rapid shifts in liquid junction potentials measured between NaCl and KCl biionic solutions [1.0 NaCl (with 145 mM NaCl) and 1.0 KCl (with 145 mM KCl); at 22°C; see Fig. 1 (main paper) and* ***Solutions*** *section for full details of solution compositions] as the difference between a 150 mM NaCl agar salt-bridge (initially equilibrated with a 1.0 NaCl solution) and a 3M KCl reference salt-bridge, when the 3M KCl salt-bridge tip is cut off just prior to every solution transfer. The black vertical bars (and bold 'C's) indicate the period during which the solution is changed and the tip of the 3M KCl reference salt-bridge was cut, thereby having a fresh 3M KCl interface in contact with the new solution.*

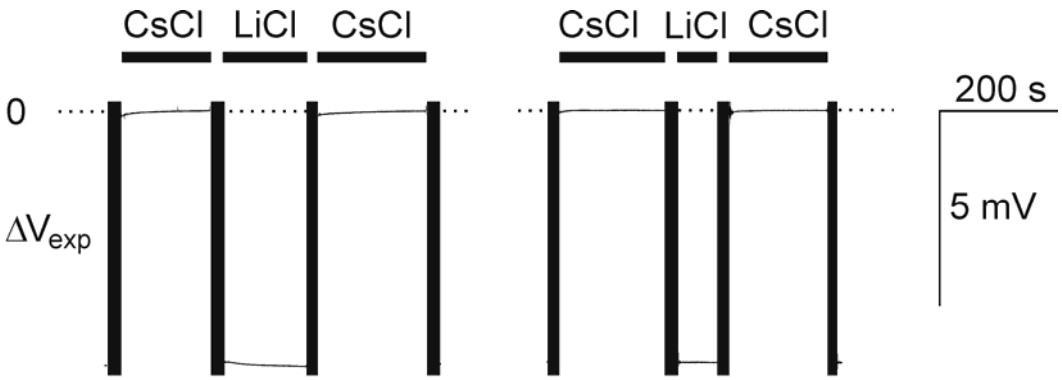

Fig. S6. *An example of the shifts in LJPs measured between CsCl and LiCl biionic solutions [1.0 CsCl (with 145 mM CsCl) and 1.0 LiCl (with 145 mM LiCl); at 22°C; as the difference between a 150 mM CsCl agar salt-bridge (initially equilibrated with a 1.0 CsCl solution) and a 3M KCl reference salt-bridge, when the 3M KCl salt-bridge tip is cut off just prior to every solution transfer (with the black vertical bars indicating the solution transfers when the 3M KCl salt-bridge is cut, as in data shown in Figs S2-S5). However, notice that when the time duration in the LiCl test solution is closer to that in the CsCl control solution (left 3 changes), there is a small initial transient component to the* ΔV_{exp} *shifts, but that when the test solution duration is relatively much shorter, the initial transient components are reduced (right 3 changes).*

Table S2. The limiting equivalent conductivities (Λ^0) of Li^+, Na^+, Cs^+ and Cl^- ions at various temperatures. The published values at 15, 18, 25 and 35 ^oC were obtained from Appendix 6.2 of Robinson and Stokes (1965). The published data at 15, 25 and 35 ^oC are reliable to within the last figure given and the 18 ^oC values to 2 or 3 units in the last figure given. The other asterisked values at 20 and 22 ^oC were fitted (using Sigma Plot 9.0) from quadratic polynomial fits to the published values at all 4 temperatures in the case of Li^+, Na^+, K^+ and Cl^- and to the 15, 25 and 35 ^oC values for Cs^+, though the 18 ^oC value did happen to be close to the fit.

Temp. \ ion (X)	Li^+	Na^+	K^+	Cs^+	Cl^-
15 ^oC	30.2	39.7	59.6	63.1	61.4
18 ^oC	32.8	42.8	63.9	67	66.0
20 ^oC*	*34.35**	*44.81**	*66.53**	*70.05**	*68.84**
21 ^oC*	*35.19**	*45.85**	*67.92**	*71.46**	*70.34**
22 ^oC*	*36.04**	*46.91**	*69.32**	*72.89**	*71.85**
25 ^oC	38.6	50.10	73.50	77.2	76.35
35 ^oC	48.0	61.5	88.2	92.1	92.2

*These values were fitted to an equation in the form ($y = y0 + at + bt^2$, where t is the temp in ^oC, y is the $\Lambda^0(t)$ used to fit them and y0, a and b are the fitting parameters, are as follows:
Li^+: y0=19.444; a=0.65114; b=0.004698; Na^+: y0=25.961; a=0.8451; b=0.004861;
K^+: y0=40.2143; a=1.2428; b=0.003651; Cs^+: y0=43.450; a=1.250; b=0.0040;
Cl^-: y0=40.6275; a=1.3276; b=0.004158.

Possible effect of electric field on Cs^+ mobility

It should be noted that a molecular dynamics study of alkali cation mobilities by Lee and Rasaiah (1994) at infinite dilution indicated that the hydrated water molecules around the alkali cations are bound in inverse proportion to their ionic radii, so that the smallest ion , Li^+ (bare ionic radius 0.068 nm), has **a** primary solvation shell of water molecules 'stuck to it and moving with it as an entity' with a residence time of about 190 ps or longer, behaving as in the classic solventberg model (see Appendix A in Sugiharto et al., 2008). For Na^+ (radius 0.097 nm) this residence time reduces to about 35 ps, whereas for the large Cs^+ ion (radius 0.167 nm) the water molecules are only loosely bound and the residence time is only about 8-11 ps. In addition, Table III in Lee and Rasaiah (1994) suggest**s** that there is a 4% decrease in the number of water molecules coordinated by Cs^+ in the presence of an extremely large electric field compared to in its complete absence, in contrast to the situation**s** for Li^+, Na^+ and K^+. If this is correct, this would seem to be compatible with a reduced u_{Cs} even in the presence of a smaller but still substantial (e.g., 12 V/cm) applied electric field, as used in the measurement of limiting equivalent conductivity. Hence, the loosely bound hydration shell is more likely to be stripped away from the ion than it would be in a much smaller or non-existent electric field, such as might occur under biionic or dilution concentration gradients. If u_{Cs}/u_K at 22 ^oC is reduced from 1.049 to about 1.040 for both CsCl biionic and dilution data, the difference between measured and predicted ΔV_{LJ}s would be reduced to within the expected ± 0.1 mV for CsCl:LiCl and CsCl:NaCl and 0.1 mV outside it for CsCl:KCl bionics and brought into exact agreement for 0.5 and 0.25 CsCl dilutions.

Calculations of concentration profiles of test solute and KCl in the '3M' KCl salt bridge due to KCl and solute diffusion between it and the bath solution (see Fig. 5 in main paper)

From Eqs. 6 and 7 in the main accompanying paper (Barry et al., 2012), and the appropriate diffusion coefficients, we can calculate the changes in concentration profiles of test solute and "3M" KCl in the salt-bridge with time. These changes for NaCl as a test solute after a cut salt-bridge has been in control solution for various conditioning times are given in Table S3 and shown in Fig. 5 of the main paper. The distance scale has been expanded in Fig. S7 for a conditioning time of 20 min (1200 sec) to more readily show the concentration changes over shorter distances for such a conditioning time. For example, in such a case at 20°C, the concentration of the NaCl test solution will have risen to 56% of its bath solution 1 mm in from the end of the salt-bridge, and the KCl solution will have dropped to about 39% of its 3M concentration at that same distance. However, at 5 mm from the end of the salt-bridge, the NaCl concentration will be only 0.3% of its bath concentration and the KCl concentration will have only dropped to 98.9% of its original 3M concentration.

Table S3. Relative concentrations at different distances from the end of a 3M KCl salt-bridge placed in a large volume of test solute with concentration C_{s0}, as a result of the diffusion of test solute into, and KCl out of, the salt bridge. C_{K0} is the initial KCl concentration in the freshly-cut 3M KCl salt-bridge at $t = 0$, and C_K and C_s are the subsequent concentrations of KCl and the test solute within that salt-bridge, respectively, at a later time, t. The values were calculated from Eqs. 5 and 6 in the accompanying paper. Diffusion coefficients were at 25°C and corrected for 4% agar in the 3M KCl salt-bridge (See also Fig. 5 in the main paper).

Time t (min)	Rel concs.	Distances in mm from end of 3M KCl salt bridge					
		0.1	1.0	5.0	10.0	20.0	30.0
5 min	C_s/C_{s0}	0.911	0.266	0.000	0.000	0.000	0.000
	C_K/C_{K0}	0.077	0.664	1.000	1.000	1.000	1.000
20 min	C_s/C_{s0}	0.956	0.578	0.005	0.000	0.000	0.000
	C_K/C_{K0}	0.038	0.370	0.984	1.000	1.000	1.000
120 min	C_s/C_{s0}	0.994	0.943	0.720	0.473	0.151	0.031
	C_K/C_{K0}	0.005	0.050	0.244	0.466	0.786	0.938

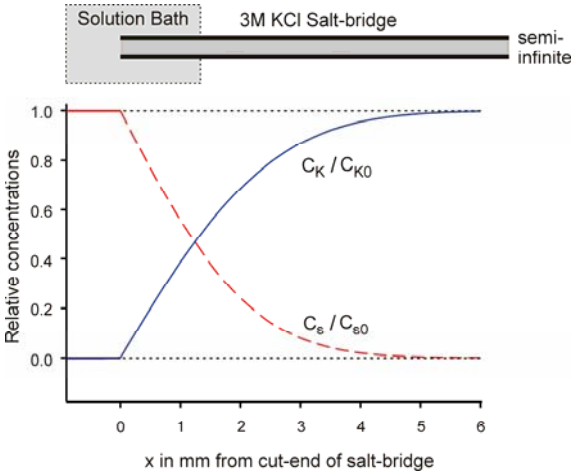

Fig. S7. *A schematic diagram to indicate the relative concentration changes at the tip of an effectively semi-infinite 3M KCl salt bridge with the cut-end placed in an NaCl salt bath. It differs from Fig. 5 (main paper) in that only the curves for a conditioning time in NaCl of 20 min are shown and in that the x axis has been expanded to more readily show the large relative concentration changes within 6 mm from the cut-end of the salt bridge over this time.*

Additional dilution experiments in simple NaCl solutions

Table S4 shows the results of some additional dilution experiments to measure LJPs for simple NaCl solutions without the addition of solutes included in the main paper measurements to represent those used in typical physiological experiments – namely, sucrose to compensate for different solution osmolalities in dilution measurements, glucose and pH buffer (e.g., HEPES and NaOH). The first two rows (150:300 NaCl) and (150:75 NaCl) can be used compare the results for similar concentration gradients, to test whether different absolute NaCl concentrations affect the agreement between measured and predicted LJPs. The second two rows (150:75 NaCl) and (150:37.5) can be used to compare the agreement between measured and predicted values in these simple NaCl solutions with the agreement between measured and predicted NaCl values in the physiologically equivalent '0.5 NaCl' and '0.25 NaCl' dilutions in Table 2 in the main paper.

Table S4: Experimental measurements of liquid junction potentials (ΔV_{LJ}^{m}) in mV at 22 ^{o}C for three simple NaCl solutions, with no added sucrose, glucose or pH buffer, and with concentrations in mM.

Control NaCl	Test NaCl	$-\Delta V_{exp}$	Using activities				n
			ΔV_{3M}	ΔV_{LJ}^{m}	ΔV_{LJ}^{p}		
150	300.0	+2.8 ± 0.01	+0.7	+3.5	+3.4		7
150	75.0	-2.9 ± 0.01	-0.6	-3.5	-3.4		6
150	37.5	-5.9 ± 0.01	-1.1	-7.0	-6.8		7

As indicated' just the calculations using ion activities are shown; m refers to measured values and p to predicted ones. All calculations used converted molality values rather than molarities, and calculation rounding errors are to within ±0.1 mV.

The results shown in the first two rows are consistent with there not being any significant (non-electrical) cross-coupling effects between the Na^+ and Cl^- ions at different absolute concentrations. The results shown in the last two rows indicate that the concentrations of sucrose used did not significantly affect the agreement between measured and predicted LJPs for NaCl dilutions and hence that such concentrations of sucrose do not appreciably affect the magnitudes of the LJPs.

Appendix S1: The relationship between generalized relative ionic mobility and limiting equivalent conductivity

by Peter H. Barry

Firstly, it should be noted that the relative mobility of an ion, u, required for calculating liquid junction potentials (as listed in the tables of mobilities in published sources and required in *JPCalc* calculations) represents the generalised (or absolute) mobility of an ion relative to K^+. For example, if u_X, is the relative mobility for ion X, with respect to K^+, it will be given by:

$$u_X = u^*_X / u^*_K \qquad \text{(S10)}$$

where u^*_X and u^*_K represent the absolute values of the generalised mobilities of ions X and K^+ respectively. The units of the relative mobility for ion X, u_X, are (of course) dimensionless.

The following discussion indicates how the generalised mobilities of ions are in turn related to their limiting equivalent conductivities.

Since the velocity of an ion in solution, v, is related to the generalised (absolute) mobility, u^*, and the generalised force, F_x, acting on it, then:

$$v = u^* F_x \tag{S11}$$

The force may be in Newtons/mole or Newtons, depending on whether it is the force acting on a mole of ions or on a single ion (and whichever is chosen will affect the units of u^*). The above generalised mobility is what is required for electrodiffusion flux equations, and would normally be that required for a force acting on a mole of ions.

In contrast, electrochemists, when measuring conductivity, use another definition of mobility, which may be defined as u', the electrical mobility, sometimes also called the 'conventional' mobility (Bockris and Reddy (1973); pp. 369-373), since they measure the mobility as the velocity/ electric field, E (e.g., in volts/m) as:

$$v = u' E \tag{S12}$$

Since the actual force referred to in Eq S11 is zFE, we also have $v = u^*|z|FE$, where $|z|$ is the magnitude of the valency and F is the Faraday. Hence we have $u' E = u^*|z|FE$ *, and:*

$$u^* = u'/|z|F \tag{S13}$$

We wish to know the relationship between generalised (absolute) mobility and the limiting equivalent conductivity, Λ^0 (the conductivity of an electrolyte solution per equivalent, in the limit as the concentration goes to zero). Now Λ^0 makes allowance for the additional charge of polyvalent ions, so that:

$$u' = \Lambda^0 /F \tag{S14}$$

[cp. equations 4.156 - 4.160 in Bockris and Reddy (1973; p.373) for equivalent conductivity (Λ) and molar conductivity (Λ_m), where $\Lambda = \Lambda_m/|z|$; Note that there is an error in sign of the anion subscript in Eq. 4.160].

Hence, from the two equations above, the generalised mobility, u^*, and Λ^0 will be related by:

$$u^* = \Lambda^0 / (|z|F^2) \tag{S15}$$

{cf. the equation for the generalized mobility, u, of a single ion, rather than a mole of ions, u^*, which is given by $u = N\Lambda^0 / (|z|F^2)$, where N is Avogadro's number (e.g., Eq. A4 in Sugiharto et al., 2008)}. Hence, the relative mobility of ion X of valency z is given by:

$$u_X = \Lambda^0_X / (|z| \cdot \Lambda^0_K) \tag{S16}$$

since, for K^+, $|z| = 1$ and both limiting equivalent conductivities were measured at the same temperature.

For a monovalent ion Y, its relative mobility will simply be given by:

$$u_Y = \Lambda^0_Y / \Lambda^0_K \tag{S17}$$

where Λ^0_Y is the limiting equivalent conductivity of Y at the same temperature as for Λ^0_K , normally 25 ^oC.

For reference, Λ^0_K = 73.50 S.cm^2.equiv^{-1} at 25 ^oC (Robinson and Stokes, 1965).

Appendix S2: The validity of the use of the Henderson equation for calculating LJPs

While the Henderson equation (Henderson, 1907, 1908; MacInnes, 1961) has proved to have been very successful in predicting experimental values of liquid junction potentials (see below), it is not a solution of the Nernst-Planck-Poisson set of electrodiffusion equations. It is based on a thermodynamic derivation of a pseudo steady-state liquid junction potential (LJP) between two liquids obtained by adding up the incremental potentials across a number of small solution layers with slightly varying compositions between two solutions because of the differences in transference (transport) numbers between each of the individual ions. The only assumption made is that each layer represents a mixture of the compositions of the two solutions initially brought into contact (see excellent discussion of the equation derivation in Chapter 13 of MacInnes, 1961). When the appropriate equations are integrated they result in Eqs. (2) and (3) presented in this paper. It should be noted that for two simple situations - a dilution potential between two uni-univalent electrolytes at different concentrations [e.g., NaCl (C_1) : NaCl (C_2); a Type 1 junction] or a biionic potential between two uni-univalent electrolytes at the same concentration but with one of the ions different [e.g., NaCl (C_1) : KCl (C_1); a Type 2 junction] the form of the equations are exactly the same as those of the simple Planck electrodiffusion equation. The latter equation is based on the steady-state solution of the Nernst-Planck electrodiffusion flux equations, with the assumption of a defined (constrained) junction region of known thickness separating the two well-stirred solutions, and the assumption of approximate local concentration "electroneutrality" of the individual local elemental regions across that junction. For a Type 1 junction this gives rise to a linear concentration gradient for both ions. As noted, the Henderson equation has been very successful in predicting experimental values of liquid junction potentials measured with Ag/AgCl (Barry & Diamond, 1970), 3M KCl pipette (Ng & Barry, 1995; Keramidas et al., 1999) and freshly-cut 3M KCl salt-bridge reference electrodes (Sugiharto et al. 2010; Barry et al, 2010) and this present paper, with the last 3 papers using increasingly more refined techniques for accurate measurement of the LJPs.

An important question is how does the Henderson equation compare with rigorous dynamic electro-diffusional theories of liquid junction potentials? As Dickinson et al. (2010) reasonably point out, for typical liquid junction potential situations with unconstrained junctions, the junction region will continue to increase in width with time and the magnitude of the slope of the ion concentration profiles will decrease with time. One basic apparent problem with the "steady-state" Henderson and Planck equations is that they assume an approximate local electroneutrality within the liquid junction region and yet clearly the LJP arises from the integration of the electric field across the junction. This electric field is generated by the differential separation of charge between cations and anions arising from the movement of cations and anions with different mobilities (and hence generally different transport numbers) down their electrochemical gradients. Clearly, when the junction region is still small and the charge separation growing, the imbalance between anions and cations over small distances can be substantial and the electric field large. As indicated by Dickinson et al. (2010), this problem was first addressed properly in the 1960-1970s. In 1965, Hafemann used a numerical computer simulation together with the principles of irreversible thermodynamics to calculate the electro-diffusion of each of the ions at a junction of two unconstrained uni-univalent electrolytes (Type 1 junction). By dividing the junction into about 100 planar elements and using an integration formulation of Gauss' law the electric field was calculated in each element generated from a summation of the charge imbalance in the other elements. He showed that for his salt dilution junction example, the LJP rapidly asymptotes to a maximum steady value, with a rise time of about 10^{-9} s, with the steady-state value agreeing with predictions of the

Henderson equation. Hickman (1970) outlined a more general, rigorous approach to this problem, using the Nernst-Planck equations and the Poisson equation (derived from Gauss's law), using perturbation techniques to generate analytical power series expansions, for multiple ionic components and even allowing for incompletely ionized systems. Importantly, he showed that the Henderson equation was the leading term in a series expansion of power terms of a small parameter, with all the other terms becoming insignificant for long times. In 1974, Jackson, refined Hickman's approach for the case of two univalent ions in a dilution liquid junction, to elucidate the underlying physical explanation of what this parameter represents and what is occurring in the LJP over such times. He provided a simple explanation of the paradox of the development of a steady potential and apparent charge electroneutrality. At any point, the charge density decreases to zero with time (t) as t^{-1}, the spread of charge increases as $t^{1/2}$, so the net charge per unit area decreases as $t^{-1/2}$. Since the potential difference is of the order of the product of the electric field (which is proportional to the charge per unit area, which goes as $t^{-1/2}$) and the separation (proportional to $t^{1/2}$ for large times), the potential difference should be constant. This indicated for such a system why the LJP should be time-independent for times greater than about 10^{-9} s (assuming reasonably that the solution boundaries may be considered to be semi-infinite for the times involved), and why the LJP is given by the Henderson equation. Recently, Perram and Styles (2006) used a numerical analysis of the Nernst-Planck-Poisson equations and perturbation theory for the liquid junction potential of a uni-univalent salt gradient (Type 1 junction) across a thick porous membrane (constrained junction) to show that the LJP initially rose rapidly and then also asymptoted to the Henderson equation.

More recently, Compton and colleagues (Dickinson et al., 2010, Ward et al., 2010 and Zhurov et al., 2011) have used a more exact and rigorous Nernst-Planck-Poisson (NPP) finite difference numerical simulation system, together with perturbation analyses, to confirm and extend the basic conclusions of the above earlier studies, and produce a complete quantitative simulation of the dynamic evolution of the liquid junction potential across an unconstrained junction, together with the evolution of the profiles of the ionic concentrations and electric field across the expanding junction region, from the moment the two different semi-infinite solutions first come into contact. Dickinson et al., (2010) in particular determined the evolution of the electric field profiles across the liquid junction for a range of different time durations for both Type 1 dilution junctions (Fig. 6) and Type 2 biionic junctions (Fig. 15). They showed that in both cases, the electric field initially rose very rapidly to a maximum in a 5-50 ns timescale with a very narrow spike profile, before reducing in height and continuing to broaden out with time as in Figs. 6 and 15. With respect to the magnitude of the LJP, they validated the previous asymptotic analyses by Hickman (1970) and Jackson (1974) and showed that the LJP rapidly rises to a maximum steady plateau value [given by $-\Delta\theta_{LJP}$ in Figs. 2 and 11 of Dickinson et al., 2010 for Type 1 (dilution) and Type 2 (biionic) junctions respectively] close to the values predicted by the Henderson equation. In their accompanying online Supporting Information C, Dickinson et al. (2010) also demonstrated strong agreement (within 0.25% in their simulations) with the Henderson equation for the LJP magnitudes ($\Delta\theta_{LJP}$) in the Type 1 junctions for a range of different cation/anion mobilities (Fig 1), with it tending to exact agreement with the Henderson equation for theoretical asymptote perturbation analyses. For Type 2 junctions, Dickinson et al. (2010) found good, but not quite so strong, agreement (within 0.8%) for $\Delta\theta_{LJP}$ for a range of different cation-cation mobilities for Type 2 junctions (Fig 2). In support of these latter results, they showed (Supporting Information H) that the asymptotic analysis of Hickman (1970) for Type 2 junctions required "…a further perturbation involving diffusion coefficients …. to achieve approximate results for this asymptote…" and so was not in exact agreement with the Henderson equation. They indicated that LJP reaches steady value "…at time scales of 10-1000 ns after junction potential formation for typical aqueous systems, by which time the diffuse layer is approximately 10-1000 nm in extent and is continually expanding …" Dickinson et al. (2010).

Ward et al. (2010) in the Compton group used the same approach to investigate Type 3 junctions (A^+X^- || B^+Y^- ; e.g., biionics with no common anion) with a multilayer liquid junction and found there could be greater deviations from the Henderson equation. Nevertheless, for the junction (KNO3 || NaCl), where there were relatively small differences in relative mobilities (1, 0.682, 0.972, 1.039 respectively; proportional to their diffusion coefficients), they calculated a very close agreement with the Henderson equation (with difference < 0.01%) for a calculated LJP of 5.37 mV for that equation. Even for the junction ($Na^+Acetate^-$ || K^+OH^-), where there are substantial differences in relative ion mobilities (0.682, 0.556, 1.0, 2.69 respectively; http://web.med.unsw.edu.au/phbsoft/mobility_listings.htm), they only observed a deviation of 1.55% from their simulated value of 20.4 mV compared to the value of 20.72 mV from the Henderson equation**.** They did indicate that when there was a much more substantial difference between the maximum and minimum relative ionic diffusion coefficients (or relative ion mobilities) the deviation from the Henderson equation could increase further and be more than 8%. They defined a small parameter $\mu = (D'_{max} - D'_{min})/(D'_{max} + D'_{min})$ as in Eq. 3.5 of their paper, where D'_{max} and D'_{min} are the maximum and minimum single ion diffusion coefficients for the four ion species in the junction. Asymptotic analysis (Hickman, 1970) resulted in the first term of an expansion being equal to the Henderson equation (for long times), with a power series of μ terms, and in relatively extreme cases, this could produce very significant deviations from the Henderson equation for Type 3 junctions. They also observed that larger deviations from the Henderson equation occurred when both the cation and anion on one side of the membrane had greater ionic diffusion coefficients, but similar to each other, than those ions on the other side of the junction (Ward et al., 2010). *It should also be appreciated that the above mobility comments are only relevant to the mobilities of the predominant four ion species in the solutions, which were all that were considered in the above cases, and that the inclusion of* ***small concentrations of*** *additional ions, which have either very low or very high mobilities, to solutions with high concentrations of more standard ions will only contribute minimally to the LJP. In addition, for almost all relevant predominant ions in physiological solutions, the range of ion mobility values would be much less than in the above KOH case.*

In summary, these informative theoretical studies on the evolution and underlying mechanisms of LJPs provide validity and a theoretical rationale for the use of the Henderson equation for calculating pseudo 'steady-state' LJPs in the double semi-infinite solution junction described above. In particular, the theoretical analyses by Compton et al. suggest that while Type 1 junctions are expected to give exact asymptotic agreement with the Henderson equation, subtle small differences between experimental LJPs and predictions of the Henderson equation may be expected with Type 2 biionic junctions (e.g., 0.8%), and greater differences with the Type 3 biionic junction (e.g., 1.55%) with greater mobility differences. These papers provide a strong theoretical basis for the validity of the Henderson equation as an approximate asymptotic estimate of the LJP for various types of junctions and indicate where significant deviations from the Henderson could occur.

Furthermore, it should also be noted that for the salt-bridge – solution bath system discussed in this present paper, the interface between a small salt-bridge in contact with a large volume bath, is likely to behave as a constrained boundary, which would tend to hold the composition at that interface close to the bath composition, whereas the salt-bridge (or pipette) would behave as a semi-infinite solution. This would result in a much simpler system than two semi-infinite solutions in contact and it seems most likely that the pseudo steady-state LJP of such a single semi-infinite junction should be even more closely approximated by the Henderson equation, maybe at least halving the above deviations. Such a system could be a worthy subject for a rigorous Nernst-Planck-Poisson analysis.

As Hafeman (1965) points out in his analysis, which is clearly true of all the above theoretical analyses discussed, none of them assumes the presence of any non-electrical cross interaction between different ion fluxes or effects due to solvent convection. Such effects have been modeled in considerable detail by Mori et al. (2011) using principles of irreversible thermodynamics to

simulate electro-diffusion and osmotic water flow across cell membranes and tissues. With respect to the differences in osmotic concentrations between the agar salt-bridges and bath solutions, it might be thought that this could give rise to some solvent flow between them. However, since the agar salt-bridges are an open porous matrix with less than a 10% drop in diffusion coefficient, it would be expected that the reflection coefficient for sucrose would be zero and that there would be no solvent flow in or out of the salt-bridges. The predicted lack of osmotic effects for salt-bridges was confirmed when dilution LJPs were measured in the absence of any osmotic sucrose compensation for NaCl solutions with dilutions to 50% and 25% concentrations, where there was also excellent agreement between measured and calculated LJPs using the Henderson equation (see ESM Table S4 in the Electronic Supplementary Material). Similarly, if cross-coupling effects were significant in such LJPs, there might be expected to be a difference between two-fold gradients at different absolute salt concentrations. However, the measured values for a simple NaCl salt gradient of 150:300 and for a 150:75 gradient were equal in magnitude, but with reversed sign (ESM Table S4), consistent with no convective effects. In addition, while there are small effects of sucrose on Ag/AgCl electrode potentials (e.g., of about 0.3 mV for 200 mM sucrose; Barry & Diamond, 1970) these are not relevant with the freshly-cut 3M KCl salt-bridge reference system technique used in this paper. However, it is known that sucrose will reduce the dielectric constant of aqueous solutions (e.g., a decrease of ~2.5% at 25 ^{o}C; Akode et al., 2004), which would tend to slightly increase the activity coefficients of all the ions in solution. Since the contribution of activity coefficients in LJPs is small anyway (see Table 2), this seems unlikely to be very significant. Another possible effect of the sucrose is on the hydration of the ions. From molecular dynamics and potential of mean force calculations on aqueous sucrose solutions of an Na-Cl ion pair, Martorana et al. (2000) have estimated that a 60% w/w (~4.4 molal) solution of sucrose will reduce the first hydration shell of Cl^{-} from 3.6 to 2.8 (22% decrease) water molecules and that of Na^{+} from 5.9 to 5.0 (15%), but since this sucrose concentration is about 22 times greater than the sucrose concentrations used in this present paper (~200 mM sucrose), the effect on relative mobilities is likely to be very small. This is shown by the LJP measurements and calculations in the presence (~190 mM sucrose) and absence of sucrose for the 0.25 NaCl dilutions (in Tables 2 and S4). These results indicate that the concentrations of sucrose used did not significantly affect the agreement between measured and predicted LJPs for NaCl dilutions and hence that such concentrations of sucrose do not appreciably affect the magnitudes of the LJPs.

However, with a pipette reference electrode, instead of a salt-bridge, in contact with a bath, if the solution in the pipette were free-flowing under a hydrostatic gradient, to minimize history-dependent effects, the resultant volume flow may have a convective effect on the magnitude of the LJP.

Appendix S3 Measurement and calculation of LJPs when ion mobilities are not known

If the mobilities of one or more of the major ions in a solution are not known accurately, then the LJP can be directly measured, but for an accurate LJP value there still needs to be a correction for the ΔV_{3M} contribution to the LJP? But how can this correction be calculated without values for all the ion mobilities? First of all, as Tables 2 and 3 in the main paper indicate, the contribution of the ΔV_{3M} term is a second order effect (e.g., there is only a 0.2 mV difference in the ΔV_{3M} term between the 0.25 dilutions of NaCl and LiCl) and only a very rough estimate of the non-KCl ion mobilities is needed (either from known mobilities of ions of a similar size and properties) in order to estimate the .ΔV_{3M} contribution to the LJP (see further discussion in ESM). It should be noted from the above tables that ΔV_{3M} is generally only a relatively small fraction of the measured LJP, except when the ion mobilities are very similar, in which case both the LJP and ΔV_{3M} are very small anyway.

If the unknown ion is one of the major ones, then trial values of that unknown ion can be iteratively tried and the corrected measured LJP value (e.g., ΔV_{LJ}^{ma} in Tables 2 and 3 or ΔV_{LJ}^{m} in

Table S4) compared with the calculated value (e.g., ΔV_{LJ}^{pa} in Tables 2 and 3 or ΔV_{LJ}^{p} in Table S4) to minimize the divergence between the two values. Indeed, LJP measurements with the above technique could be used in simple uni-univalent salt dilution measurements, for an ion with unknown mobility in combination with a counterion of known mobility, to at least estimate the mobility of the first ion, without having to do limiting equivalent conductivity measurements.

References

Barry PH, Lewis TM, Moorhouse AJ (2012) An optimised 3M KCl salt-bridge technique used to measure and validate theoretical liquid junction potential values in patch-clamping and electrophysiology, Eur Biophys J (submitted)

Barry PH, Sugiharto S, Lewis TM, Moorhouse AJ (2010) Further analysis of counterion permeation through anion-selective glycine receptor channels. Channels 4:142-149

Bockris JO'M, Reddy AKN (1973). Modern Electrochemistry, Vol 1, Plenum Press, New York

Cui R-F, Hu M-C, Jin L-H, Li S-N, Jiang Y-C, Xia S-P (2007). Activity coefficients of rubidium chloride and cesium chloride in methanol-water mixtures and a comparative study of Pitzer and Pitzer-Simonson-Clegg models (298.15 K). Fluid Phase Equilibr 251:137-144.

Dickinson EJF, Freitag L, Compton RG (2010) Dynamic theory of liquid junction potentials. J Phys Chem 114:187-197

Hafemann DR (1965) Charge separation in liquid junctions. J Phys Chem 69:4226-4231

Henderson P (1907) Zur thermodynamic der Flüssigkeitsketten. Z Phys Chem 59:118-127

Henderson P (1908) Zur thermodynamic der Flüssigkeitsketten. Z Phys Chem 63:325-345

Hickman HJ (1970) The liquid junction potential - the free solution junction. Chem Eng Sci 25:381-398

Ives DJG, Janz GJ (1961). Reference Electrodes. Academic Press, New York

Jackson JL (1974) Charge neutrality in electrolyte solutions and the liquid junction potential. J Phys Chem 78:2060-2064

Lee HL, Rasaiah JC (1994). Molecular dynamics simulation of ionic mobility. I. Alkali metal cations in water at 25 ^{o}C. J Chem Phys 101: 6964-6974.

MacInnes DA (1961) The Principles of Electrochemistry. Dover Publications, Inc. New York

Mori Y, Liu C, Eisenberg RS (2011) A model of electrodiffusion and osmotic water flow and its energetic structure. Physica D 240: 1835-1852

Perram JW, Stiles PJ (2006) On the nature of liquid junction and membrane potentials. Phys Chem Chem Phys 8:4200-4213

Robinson RA, Stokes RH (1965) Electrolyte Solutions, 2nd Ed. Revised. Butterworths. London.

Sugiharto S, Lewis TM, Moorhouse AJ, Schofield PR, Barry PH (2008). Anion-cation permeability correlates with hydrated counter-ion size in glycine receptor channels. Biophys J 95:4698-4715.

Sugiharto S, Carland JE, Lewis TM, Moorhouse AJ, Barry PH (2010). External divalent cations increase anion-cation permeability ratio in glycine receptor channels. Pflügers Arch 460: 131-152.

Ward KR, Dickinson EJF, Compton RG (2010) Dynamic theory of type 3 liquid junction potentials: formation of multilayer liquid junctions. J. Phys Chem B 114: 4521–4528

Zhurov K, Dickinson EJF, Compton RG (2011) Dynamics of ion transfer potentials at liquid-liquid interfaces: the case of multiple species. 115: 12429–12440